THE AMERICAN MINERALOGIST

JOURNAL OF THE MINERALOGICAL SOCIETY OF AMERICA

Vol. 31 MARCH-APRIL, 1946 Nos. 3 and 4

THE LOCALIZATION OF URANIUM AND THORIUM MINERALS IN POLISHED SECTION

PART 1: THE ALPHA RAY EMISSION PATTERN

HERMAN YAGODA, *National Institute of Health, Industrial Hygiene Research Laboratory, Bethesda, Maryland.*

CONTENTS

ABSTRACT

Uranium and thorium minerals occurring in polished sections are characterized by means of a selective alpha ray emission pattern on light desensitized emulsions. The characteristics and special processing of the emulsion are described. Comparative studies reveal lack of sensitivity to beta and gamma radiations, visible and ultra violet light and chemical agents producing pseudophotographic effects. The emulsion is only slightly sensitive to *x*-rays and neutron radiations. The emulsions exhibit a marked fading of the latent image on delayed development, and the latent image is destroyed by the presence of mercury vapor during the exposure. The medium produces a sharply defined, reproducible

image of alpha radiation originating from polished sections in direct contact with the emulsion. The resultant pattern can be enlarged up to 200 diameters and is serviceable in the identification of fine mineral grains and reveals the variation in the alpha ray activity of minute structures. The blackening is proportional to the number of alpha rays escaping from unit area of polished surface per second: $P_\alpha=\psi(30.1\ U+13.7\ Th)$, where ψ is the permeability of the mineral to alpha radiation and U and Th represent the quantity of uranium and thorium per gram of mineral. The radioactive minerals are classified into seven groups based on the relative photographic densities produced by the species compared with a unit of minerals of known alpha ray activity.

Introduction

Selective physical properties of matter are of considerable aid in the identification and localization of the components of a polished surface by means of analytical patterns (94). The autoradiographic pattern is of particular selectivity, as in naturally occurring substances a positive print is furnished only by the uranium and thorium minerals.[1] Shortly after the discovery by Henri Becquerel (5) that uranium compounds emitted radiations capable of penetrating black paper and rendering photographic emulsions developable, numerous investigations were reported on the photographic action of the uranium and thorium-bearing minerals. In 1900 Sir William Crookes (14) published a list of 16 minerals that activated the photographic plate and concluded: "after going through every mineral in my cabinet, a somewhat extensive collection, numbering many fine specimens" that only uranium and thorium bearing species gave the reaction. Similar studies were made by Pisani (72), who failing to interpose a black paper between the emulsion and the specimen, erroneously included wurtzite, fluorite and chlorophane in his list of radioactive minerals. These minerals are now known to be photoluminescent after excitation by sunlight, and the activation of the emulsion is caused by their persistent phosphorescence. Tables of the radioactive minerals, published by Bardet (4) and Wherry (91), were arranged in accordance with their relative photographic action, correlated with the uranium and thorium content. The autoradiographic technique is a well established tool in petrography and is employed extensively in the study of the homogeneity of specimens prior to analysis for age determinations (45).

[1] Isotopes of certain elements (potassium K^{40}, rubidium Rb^{87}, samarium Sm^{148}, and lutecium Lu^{176}) are also unstable and their spontaneous decomposition is likewise accompanied by radioactive radiations. K^{40}, Rb^{87}, and Lu^{176} give rise to beta radiation, and Sm^{148} is an alpha ray emitter. The intensity of these radiations in naturally occurring substances is very low and they can be detected photographically only by prolonging the exposure from several months to a year. By employing fast emulsions, a definite image is produced by uraninite after one hour's exposure. Hence, the potential interference of these feebly radioactive elements can be eliminated by proper control of the exposure.

The autoradiographic pattern has also been employed in studying the distribution of ingested naturally radioactive elements employed as tracers in animal tissue (6, 24, 47), in the orientation of minor radioactive constituents in crystals (34, 35), in the field of metallurgy (32, 84, 91), and in the study of radiocolloid aggregates (92). The technique has received considerable impetus since the discovery of methods for the synthesis of radioactive isotopes of elements of low atomic weight. Applications have been particularly numerous in the field of histochemistry with reference to the localization of ingested radioactive phosphorus (54), iodine (36), calcium and strontium (71). A new radiographic approach to the study of polished mineral surfaces has been described by Goodman (29, 30), in which certain constituents are rendered radioactive by neutron bombardment and the areas are subsequently localized by autoradiography.

In view of the numerous applications of the autoradiographic method, a systematic study of the technique was undertaken to define conditions for the rendition of a sharply defined pattern capable of sufficient magnification for the resolution of fine detail, and to investigate interferences with its specificity by other components in the section that are either photoluminescent or capable of producing pseudophotographic effects. Experiments with different types of plates revealed that for alpha ray emitters selective patterns can be obtained that permit the classification of uranium and thorium minerals according to alpha ray activity per unit area of (polished) surface. Since recent developments in the field of nuclear physics have given rise to renewed interest in the geochemistry of uranium and thorium, the working details of the alpha ray pattern are of timely interest to mineralogists and petrographers. The present work is confined to a description of the alpha ray pattern as a primary step in the determination of the presence of uranium and thorium in the polished section. Work is in progress on the further differentiation of the radioactive minerals by means of chemical patterns (94, 96) and will be published later.

Autoradiographic Mechanism

In the decay of uranium, thorium, and their radioactive equilibrium products, three distinct types of radiation are emitted, all of which are capable of activating photographic emulsions in varying degrees. According to Rutherford (74) the alpha, beta, and gamma rays produce in each case a marked action on the photographic plate, but owing to the difference in the absorption of these rays in the gelatin emulsion, it is difficult to make any quantitative comparison of their individual effects. Of the three radiations the alpha ray produces the most localized

ionization, and Kinoshita (44) has demonstrated that in the case of the homogeneous alpha particles emitted from Radium C′ each particle produces a detectable photographic effect. However, the alpha particle has the shortest range and is stopped after traversing through about 30 microns of a silicate mineral. Most of the beta rays are absorbed in 5 mm. of aluminum or 1 mm. of lead and probably have an average range of 3 mm. in most silicate rocks. The gamma radiations are the most penetrating of all.

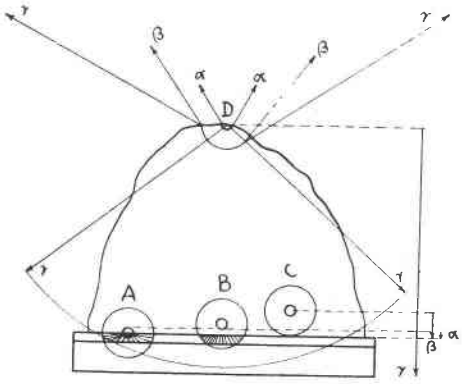

FIG. 1. Diagrammatic representation of relative photographic action of radioactive radiations on the normal type photographic emulsion.

The smallest circles represent the relative range of the alpha rays. The large circles about points A, B and C represent the active range of the beta radiation. The gamma rays originate from all parts of the mineral but are depicted only for the remote point D of the mineral.

The photographic action of the radiations is exhibited graphically in Fig. 1, showing a cross section of a massive radioactive mineral whose polished surface is in direct contact with the recording emulsion. The radiations are emitted in all directions, and each minute grain whose atoms are undergoing radioactive decomposition may be visualized as the center of a series of concentric spheres of radii equal to the range of the several radiations in the medium. Wherever these statistical spheres intersect the plane of the emulsion, the plate is rendered developable. A nucleus located directly on the polished surface, point A, will form a sharply defined image of a diameter equal to twice the range of the most penetrating alpha particle in the gelatin emulsion, accompanied by a diffuse image from the more penetrating but less active beta and gamma rays. Radioactive nuclei slightly beyond the range of the alpha particle in the mineral, points B to C, will contribute only to the fogging of the

primary pattern, and a diffuse image will be recorded on some emulsions by the gamma radiation from the most remote nuclei, point D.

It is evident from these considerations that the autoradiographic print produced on an emulsion sensitive to all three radiations is not a true representation of the uranium and thorium content of the polished surface. In experimental practice, it is necessary with ordinary emulsions to interpose a sheet of black paper between the specimen and the plate in order to avoid activation of the emulsion by phosphorescent minerals and fogging of the plate from traces of vapor escaping from the mounting media, such as balsam, sealing wax, and to a lesser extent bakelite.[2] The black paper absorbs the greater part of the energy of the alpha particles and the diffuse image formed essentially by the beta and gamma radiations can no longer be interpreted as an analytical pattern of the polished surface.

To obtain a radiographic imprint which is a true representation of the uranium and thorium content of the surface, it is necessary to arrange the experimental conditions so that only the alpha rays reach the emulsion. Direct measurements of the range of alpha particles in uranium and thorium minerals are not available, but may be approximated with the aid of the Bragg-Kleeman stopping power rule (10) which states that the energy spent by an alpha particle in its passage through an elementary atomic matrix is proportional to the square root of the atomic weight. If a mineral be composed of atoms A, B, C $\cdots$, in the relative proportions a, b, c $\cdots$, then the range of a given alpha ray, R, is closely approximated by the expression:

$$(1) \qquad R = \left[\frac{a\sqrt{W_A} + b\sqrt{W_B} + c\sqrt{W_C} + \cdots}{\rho}\right] k = \frac{\psi k}{\rho}.$$

In this equation W represents the atomic weight of the component atom, ρ the density of the mineral and k is a constant for an alpha ray of given origin. The factor ψ which varies with the chemical composition of the mineral, can be visualized as the permeability of the matrix to alpha radiation. For the alpha rays emitted by Ra C′, k can be evaluated from measurements of the radius of pleochroic haloes in biotite as recorded by Holmes (38) and is found equal to 0.00215 cm. The range in the solid of all other alpha particles originating from the disintegration of uranium, thorium, and their equilibrium products can then be estimated by multiplying k by the ratio of the range of the particular alpha ray in air to that of Ra C′ in air.

[2] The literature on this subject is very extensive. Data pertinent to mounting media can be found in references 11, 13, 63, 73, 81, 85.

Table 1 shows the variation of range of the two most penetrating alpha rays, RaC′ and ThC′, in some of the more common uranium and thorium minerals, as evaluated from equation (1) using the air range data tabulated by Rutherford (74). These computations show that only those alpha rays emitted from nuclei located on the average less than 0.004 cm. above the polished surface can emerge and have sufficient residual

TABLE 1. ALPHA RAY EMISSION FROM MORE COMMON URANIUM AND THORIUM MINERALS

Mineral	Avg. Sp. Gr.	Avg. ψ	Thickness of Active Section in microns		Escaping Rays, P_α per sq. cm. per sec.	
			Ra C′ ray	Th C′ ray	Max. P_α	Min. P_α
Uraninite	9.0	13.5	32	40	338	271
Bröggerite	9.0	13.2	32	40	273	244
Cleveite	7.5	12.5	36	45	229	207
Pitchblende*	7.0	12.5	38	—	278	246*
Thorianite	9.4	13.3	30	37	182	151
Gummite	5.1	11.5	49	—	238	171
Clarkeite	6.4	12.4	42	—	254	—
Curite	7.2	13.0	39	—	243	236
Carnotite	4.1	9.8	51	—	167	107
Torbernite	3.5	10.0	61	—	156	139
Uranophane	3.8	9.9	56	—	177	124
Uranothorite	5.3	9.7	39	48	102	60
Betafite	4.3	8.8	44	54	60	51
Samarskite	5.7	9.2	35	43	29	14
Pyrochlore	4.2	7.6	39	48	9	0
Microlite	6.4	10.2	34	42	12	0
Euxenite	5.2	8.7	36	45	23	6
Polycrase	5.0	8.3	36	45	27	16
Eschynite	5.2	8.8	—	45	19	12
Priorite	5.0	8.0	34	42	17	2
Monazite	5.1	9.2	—	48	16	7
Allanite	3.5	6.3	39	48	3	1

* These figures represent the constants of pure pitchblende. The more common crude ores are dispersions of the mineral in a siliceous matrix and the P_α of the system may run as low as 100 alpha rays per sq. cm. per sec. as indicated by Marble's analysis (55) of Great Bear Lake pitchblende.

energy to activate the emulsion. Any mechanism which can exclusively record this superficial layer of alpha ray activity will then provide a pattern closely approximating the composition of the polished surface.

An obvious approach to this mechanism is to prepare a parallel-faced slab of the specimen, slightly thicker than the range of the most penetrating alpha ray in the material. The photographic activity of the

beta and gamma radiation from a section 100 microns thick is only a minor fraction of the total, and the developed image can then be interpreted as essentially an alpha ray pattern. This method, however, fails when a black paper is interposed between the surface and the emulsion, as any filter which stops luminous rays and prevents access of activating vapors will also absorb the greater part of the alpha rays.

A solution to this problem was found in the work of Blau (8) and Wambacher (90), who discovered that when silver halide emulsions were bathed in a solution of pinacryptol yellow they lost their sensitivity for visible light, beta, and gamma radiations, but could still be activated by impact with massive nuclear particles such as the alpha ray and the proton. The wide application of these special emulsions in the field of nuclear physics (79) led to the development of improved "alpha particle plates" by the photographic laboratories of both Ilford (93) and Eastman Kodak (20), and these plates are now available as regular commercial items. The Eastman fine grained alpha particle plate has been employed by Tyler and Marais (87) in the determination of the relative radioactivity of mineral grains by counting the number of alpha tracks developed about each particle embedded in the emulsion. More recently, Baranov and co-workers (3) have described the application of similar light desensitized thick-layered photographic emulsions in the distribution of traces of radioactive matter in carbonate and carbonaceous rocks. Trial autoradiographs with these emulsions showed that although a sharp image developed after contact with a polished section containing uranium and thorium minerals, the density was low and of poor reproducibility using the conditions of development recommended for the registration of individual alpha ray tracks. Further studies led to the method of development here described, which yields images of satisfactory density and reproducibility without destroying the specificity of the emulsion for alpha rays.

Properties of Alpha Particle Emulsion

The Eastman alpha particle plates employed in these investigations consist of a thick layer of fine-grained silver halides desensitized to light. In order to absorb the high energy alpha rays emitted by Ra C′ and Th C′ impinging perpendicularly on the plate, the emulsion layer must have a thickness in excess of 50 microns. It is difficult to secure uniform development of these thick emulsions when the developing solution is kept at the customary temperature of 20°C. Neither altering the time of immersion, nor adding gelatin softeners to the developer gave reproducible autoradiographic images. After numerous trials, satisfactory results were obtained by simply warming the developing solution (East-

man D-19) to 32°C. At this elevated temperature, the latent image is rendered visible a few seconds after the plate is immersed into the bath and development is completed in two minutes. When the plates were developed at the standard temperature of 20°C., the densities of the images were very erratic on successive exposures to the identical source of alpha radiations. By developing at 32°C., the density of the image was reproducible on repeated trial, and was proportional to the exposure. By this unorthodox developing procedure, the emulsions were investigated for interferences with their specificity as recording media for alpha rays.

Action of Light:—The emulsions are remarkably insensitive to visible and ultraviolet light. Plates were covered with a coin and exposed at a distance of 10 feet for five minutes to the light from a 100 watt tungsten filament bulb and a cold quartz mercury vapor lamp. Only with the ultraviolet illumination did a faint fog develop on the area of the plate unprotected by the coin. Persistently phosphorescent minerals (antozonite, wurtzite) were excited to strong luminescence and placed in direct contact with the emulsion for periods varying between 5 minutes and 30 days. In no experiment was an image produced on development of the alpha particle plate. Under the same conditions of excitation, the specimens produced black images only after two minute periods of contact with *x*-ray or panchromatic emulsions (94).

Action of Pseudophotographic Agents:—An alpha ray plate was exposed to the vapors escaping from a 3% hydrogen peroxide solution for 30 minutes. No trace of blackening appeared on development. Under the same conditions, a deep black image developed when a contrast lantern slide emulsion was exposed to the vapors for an equal period. The traces of hydrogen peroxide formed by the oxidation of mounting media (bakelite, Wood's metal, montan wax) have no effect on the alpha ray emulsion even when the exposure is prolonged to 30 days. When the wooden contact camera is employed shortly after its preparation, the vapors arising from the sanded surface produce a very faint fog on the portions of the alpha ray emulsion not covered by the specimens. This effect is of diminishing intensity as the wood ages. Distinct pseudophotographic images caused by the mounting media are readily observable after 3 day exposures when using process or lantern slide emulsions as autoradiographic media.

Effect of Pressure:—Recent studies on the development of a latent image by pressure (2) on ordinary silver halide emulsions show that pressures of about 1000 kg. per sq. cm. must be employed to produce a measurable effect. When a polished surface is placed in contact with the emul-

sion, the weight of the specimen is uniformly distributed and the pressure at any given point of contact is low even when the specimen is clamped to the plate to prevent possible movement during exposure. Under the experimental conditions of exposure, no images were produced by direct contact of non-radioactive, polished specimens of equal weight and surface area.

Chemical Reactions with the Emulsion:—Since the polished surface of the specimen is in direct contact with the emulsion, the possibility of chemical reactions between certain minerals and the silver halides must be considered. A side reaction might arise between sulfide minerals and the silver salts in the emulsion. However, close examination of the plate after 30 day periods of contact with several common sulfide minerals (pyrite, chalcopyrite, chalcocite, pyrrhotite, pentlandite) and native sulfur showed complete absence of a brown image of silver sulfide. Mercury vapor will destroy the sensitivity of the emulsion to alpha radiations. However, native mercury is not known to occur with uranium or thorium ores.

Effect of Beta and Gamma Radiations:—In order to avoid long exposures in studying the properties of the fine-grain alpha particle emulsions, a more concentrated source of radiations than that afforded by uraninite was employed. This was prepared by dissolving 100 grams of uraninite in nitric acid and co-precipitating the radium onto about 200 mgs. of barium sulfate. This concentrate was deposited as a thin film on a brass disk and the emulsions were exposed to the radiations at a distance of 3 mm. from the film source. All quantitative measurements of photographic activity were made about two months after the preparation of the source in order to permit the radon to regain its normal equilibrium concentration.

Direct exposure to the source for 15 minutes produced an image with a photographic density of 0.10. When an aluminum foil of sufficient thickness to stop the alpha rays originating from RaC′ was interposed between the source and the emulsion, no image was produced after 24 hours exposure. This experiment showed that the plate was not activated by the beta and gamma radiations produced during the disintegration of radium and its equilibrium products. Further proof of the specificity of the emulsion for alpha rays was secured by exposing a series of four slabs cut from a single specimen of practically homogeneous uraninite. After polishing, the heights of these slabs were approximately 10, 5, 1 and 0.1 mm., respectively. On development, after a 100 hour period of exposure, the four images appeared to be equally black and subsequent measurement revealed only a maximum variation of 5 per

cent in photographic density between the 10 mm. and the 0.1 mm. sections.

Effect of X-ray Radiation:—An alpha particle emulsion covered with a sheet of black paper was exposed for one hour to a beam of unfiltered x-rays generated from a copper target operating at 35,000 volts and 15 milliamperes. On development the image had a photographic density of 1.0. Using the normal x-ray emulsions a similar blackening is produced after 5–10 sec. exposure. This slight sensitivity of the alpha particle emulsion is of moment only in regard to its storage or exposure in proximity to x-ray machines. The spontaneous emission by minerals of radiations in the x-ray region has not yet been observed.

Effect of Neutron Radiation:—Alpha particle plates covered by black paper were exposed to slow and fast neutrons (together with the accompanying beta and gamma radiations) generated by the cyclotron at the Carnegie Institute of Washington. An exposure of 6 hours at an average current of 150 microamperes produced only a faint fog on the developed plates. Preliminary experiments indicate that boron and lithium can be localized in polished section by contacting the surface with an alpha ray emulsion and exposing the unit to neutrons. Both elements absorb neutrons with the selective reemission of alpha particles and these are recorded simultaneously by the emulsion.

Fading of the Latent Alpha Ray Image:—A very marked fading of the latent image was observed following delayed development in an effort to secure data on the relation between time of exposure and the photographic density. A polished specimen of uraninite was exposed against different portions of the same plate for periods of 1, 2, 5, 24, 48 and 377 hours. At the termination of the last exposure the plate was developed immediately after the removal of the specimen from its last position. Only two images appeared. A very dense one, corresponding to an exposure of 377 hours without delayed development, and a very faint image, corresponding to the region exposed for 48 hours and whose development was delayed for 377 hours, appeared. The remaining four portions of the plate showed no visible image. Exposures of 1 to 48 hours with the same specimen yielded distinctly visible radiographs of increasing density when the plates were developed immediately after the exposure.

To check this unusual phenomenon[3] a large sized alpha particle emulsion was cut into a series of test units. All strips received identical ex-

[3] According to Neblette (66) the latent image produced by light on ordinary photographic emulsions is extremely persistent and successful development of negatives 30 years after the exposure has been reported.

posures except that development of one set was delayed. Table 2 shows that the 20 day delay resulted in almost complete loss of the image. Each test unit was developed individually in fresh portions of the same developer at the same temperature. Measurement of the density showed that in each case delayed development caused a diminution in the intensity of the alpha ray image and that a delay of 20 days resulted in its practically complete obliteration (Table 2).

TABLE 2. FADING OF LATENT ALPHA RAY IMAGE

Photographic Density		Interval of Delayed	$(D_0-D_f)/D_0$
Undelayed D_0	Delayed D_f	Development	
0.430	0.390	1 day	0.093
0.480	0.380	2	0.208
0.430	0.275	3	0.361
0.430	0.200	5	0.535
0.400	0.140	10	0.650
0.435	0.045	20	0.896

A survey of the literature revealed that this phenomenon had previously been observed by other investigators using fine-grained emulsions treated with pinacryptol yellow. Blau and Wambacher (9) state that after 14 days the density is half that produced on undelayed development. Lauda (51), who studied the effect in considerable detail, concludes that after a 160 day delay in development the loss in density is 80 per cent when the plate is stored under ambient conditions, 60 per cent when the emulsion is kept at 0°C., and only 8 per cent when the emulsion is kept in an evacuated desiccator.

This effect is of little moment in the practical application of the emulsions in autoradiography as development can be arranged to take place without appreciable delay. It raises the question, however, whether a fading effect occurs during long period exposure to weak alpha ray sources. Experiments with the same specimen, varying the time of exposure on individually developed plates result in images of progressively increasing density. Thus, a polished section of samarskite yielded images having photographic densities of 0.33 and 0.69 after exposures of 15 and 30 days, respectively. This indicates the absence of any pronounced fading of the latent image during prolonged exposure. It is difficult to reconcile the absence of a fading effect during prolonged exposure with the pronounced fading observed on delayed development.

Effect of Mercury Vapor:—In an effort to increase the sensitivity of the fine-grained alpha particle emulsion and thereby diminish the time of exposure for the registration of an image from feebly radioactive minerals, a globule of mercury was introduced in the box holding plate

and specimen. Dersch and Dürr (18) have demonstrated that traces of mercury vapor hypersensitized panchromatic emulsions, causing an increase in speed of 75 to 150 per cent. For the alpha particle emulsion, the mercury vapor had the opposite effect, and no image appeared after development. Confirmatory evidence of the desensitization of the emulsion for alpha particles by mercury vapor was secured by supporting a plate for 40 hours in a jar containing a globule of mercury. A two hour exposure to the barium-radium sulfate source yielded on development a faint image having a photographic density of 0.02. A control plate, which did not come in contact with mercury vapor, gave the normal density of 0.43. In view of these observations, proper attention must be given to the storage of the fine-grained alpha particle plates. To avoid accidental access of vapor to the emulsion during long exposures, it is good practice to keep the specimen and plate in a desiccator.

Effect of Temperature During Exposure:—The intensity of the alpha ray pattern is not altered by small variations in temperature of the emulsion during the exposure. In one experiment the exposure (100 hours) was conducted in a refrigerator at 5°C. and the density of the plate was identical to that obtained at 25°C.

These studies show that the fine-grained alpha particle emulsion is a

FIG. 2. Comparison of autoradiographs produced by different techniques.

Specimen is an unmounted slab of crytolite containing small inclusions of gummite and a layer of uraninite on extreme right. Sample collected at English Knob Mine, Spruce Pine, N. C., by F. A. Lewis. Prints A, B, and C were full sized positive prints of original negatives (reduced ½ in reproduction).

(*A*) Eastman type II-O spectrographic plate with layer of black paper interposed between emulsion and polished surface.

(*B*) Same emulsion as *A*, but black paper omitted. Better definition is secured, but pattern is not selective owing to potential actinic interferences.

(*C*) Eastman fine-grain alpha particle emulsion. The gummite inclusions are sharply defined and a non-radioactive inclusion in the uraninite is revealed. The faint halo about the uraninite region is caused by scattering of alpha rays from exposed inclined surface of the unmounted slab. In a mounted specimen this side radiation is completely absorbed by the casing.

highly selective medium for recording the distribution of alpha ray activity emanating from a polished mineral surface. The pattern is sharply defined since the penetrating beta and gamma radiations are not recorded on the emulsion. This is illustrated in Fig. 2 where the alpha ray pattern (print *C*) is compared with an autoradiograph (print *B*) on an emulsion sensitive to all three radioactive radiations. Since the fine-grained alpha particle emulsion is not activated by visible and ultra-violet light and not subject to pseudophotographic effects, there is no need for introducing a black paper filter to achieve specificity. The advantages in clarity and resolution gained by the elimination of the filter are evident by inspection of prints *A* and *C* of Fig. 2.

Preparation of the Polished Section

The standard method for preparing polished plane surfaces by moulding the specimen in bakelite is entirely satisfactory for use in obtaining the alpha ray pattern. Specimens composed essentially of radioactive minerals are usually friable and it is good practice to reinforce the massive sample with bakelite varnish or wax prior to cutting and mounting. Minerals in the metamict state have a tendency to shatter when mounted in bakelite at a temperature of 160°C. and 3000 lbs. per sq. inch pressure. This difficulty has been encountered with massive samples of samarskite and euxenite. Little if any fissuring occurs when these minerals are mounted in montan wax. The heat treatment inherent in these procedures probably causes the loss of some radon and thoron. Comparative alpha ray patterns of freshly mounted specimens and ones which have aged sufficiently since mounting for restoration of equilibrium with the gaseous emanations show but little variation in photographic density when the plates are examined visually. In one experiment designed to test the magnitude of this factor, the images produced by a freshly mounted crystal of thorianite and the same crystal exposed a month later showed a change in photographic density from 0.445 to 0.465. This 4.3 per cent increase is undoubtedly due to restoration of thoron and radon which were lost during mounting and polishing, as a completely equilibrated control section of uraninite exposed on the same plates for an equal period of time produced images varying in density by only 0.5 per cent. It is usually not practical to age the polished section prior to its autoradiography. However, a 5 per cent difference in photographic density is difficult to see, and as the group divisions differ by 30–50 per cent, this factor is not a serious detriment to the grouping by means of a set of equilibrated standards of the radioactive minerals minerals proposed in Table 3.

Bleached montan wax[4] is serviceable both as a binder and mounting medium for friable radioactive ores. This material melts at about 85°C. to a mobile liquid, which is rapidly absorbed by porous specimens, solidifies with little change of volume, and is sufficiently hard for dry polishing on emery papers. Unlike sealing wax, montan wax does not produce pseudophotographic effects and does not flow during spells of warm weather. Specimens prepared seven years ago show no evidence of deterioration. Satisfactory polished sections of extremely crumbly material, such as deposits of partially cemented carnotite on sandstone, have been prepared successfully by the following procedure.

Melt a sufficient quantity of wax in a 50 ml. beaker to cover the specimen, heat to about 110° C. and place beneath a bell jar. Apply suction until gases cease to escape from specimen. Remove the impregnated material while wax is molten and place on a small piece of flat board in a position oriented for cutting. Allow warm wax to drip onto the specimen until it is completely covered and cemented to the board. Cut into slabs, passing cutting wheel through board and specimen. Detach slices from support, wash and wipe dry. Center a selected slab beneath a plastic screw cap as described in Fig. 3 and place the assembled press on a warm hot plate until the wax surrounding the slab begins to melt. Remove from the hot plate, fill screw cap with molten wax and allow to cool to room temperature. Remove aluminum backing (*a*, Fig. 3) by warming momentarily on a hot plate. Polish on successively finer grades of metallographic emery papers, starting with grit no. 2 and finishing with no. 0000. Any abrasive adhering to the wax is removed by moistening the last sheet of paper and rubbing the specimen in the rouge slurry. If it is desired to preserve water soluble components, the wax can be cleaned by rubbing the surface against a sheet of blotting paper.

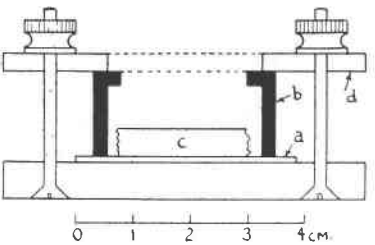

FIG. 3. Apparatus for mounting minerals in wax.

(*a*) Flat aluminum sheet about 1 mm. thick.
(*b*) Plastic shell container. A bakelite screw cap of suitable dimensions drilled with a 15 mm. hole may be employed, or the shell can be moulded to conform to standard size bakelite mountings.
(*c*) Slab of mineral impregnated with wax.
(*d*) Brass plate with hole in center for admission of molten wax.

[4] The supply of montan wax was originally obtained from the I. G. Farben Ind. and is no longer available. Domestic montan waxes exhibit a minute shrinkage on solidification, and while satisfactory as an impregnating medium, are not serviceable for mounting in screw caps. Halowax no. 2025 furnished by the Halowax Corp., N. Y. C., is satisfactory both as an impregnant and as a mounting medium.

Wood's metal of melting point 66°C. is also a satisfactory mounting medium in preparing specimens for autoradiography. It is much harder than montan wax and permits better polishing of the extreme edge of the specimen, particularly when the section contains hard ingredients. Wood's metal is attacked by etching media employed in contact printing, hence the use of this medium is limited to specimens to be employed solely as comparative standards for alpha ray activity.

After being mounted and polished, the specimen should be carefully washed with a moist piece of absorbent cotton to remove mineral dust embedded superficially on the mounting medium during the polishing process. Any linters adhering to the surface as a result of drying with soft tissue paper should be removed with a fine hair brush prior to making contact with the emulsion.

The Autoradiographic Exposure

The fine grained alpha particle emulsions are available in almost all of the standardized size photographic plates (20). The size of the plate selected should be considerably larger than the area of the specimen as the emulsion layer tends to thin out towards the edges of the plate and perfect contact with the polished surface can be effected only in the central flat portion. The mounted specimen and the annular ring containing embedded chips of known radioactive minerals are placed directly on the emulsion and both are clamped in position as shown in Fig. 4. The unit is wrapped in black photographic paper and stored in a desiccator.[5]

An exposure of 100 hours will suffice for the development of readily discernible images for minerals having a uranium content between 70 and 2 per cent. A smaller concentration of uranium and thorium can be localized by prolonging the period of contact. When the exposure exceeds 200 hours, the images produced by minerals of high alpha ray activity will be too black for accurate measurement of their photographic density. Hence, search for mineral grains of low alpha ray activity should be made on a separate plate, prolonging the exposure to 1000 hours.

[5] The primary purpose of the desiccator is to avoid contamination by mercury vapor. It has been observed, however, that excessive humidity during the exposure causes a marked lowering in the density of the developed image. This is avoided by placing a dish of calcium chloride in the desiccator. The vessel should not be evacuated, as there is danger of disturbing the radon equilibrium, and the gelatin tends to peel from the glass backing when subject to prolonged reduced pressure.

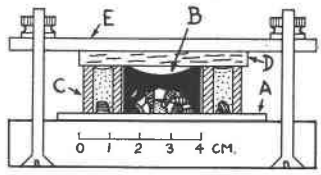

FIG. 4. Cross-section of autoradiographic camera.

(*A*) Fine grain alpha particle plate resting on wooden base.
(*B*) Mounted specimen.
(*C*) Annular lucite ring drilled with 7 holes, 5 mm. in diameter, in which are embedded chips of radioactive minerals of known alpha ray activity.
(*D*) Cotton or felt pad for equalizing pressure.
(*E*) Clamping board preventing movement of specimens during exposure.

DEVELOPMENT OF ALPHA PARTICLE EMULSION

Except for the extraordinary temperature of the developing bath, the photographic processing of the alpha particle emulsion is similar to that of light sensitive plates or films. Insoluble particles are readily embedded in the gelatin film and interfere with the subsequent photomicrography of the alpha ray pattern. Hence all solutions and wash waters coming in contact with the emulsion should be filtered, and the plate finally dried in an atmosphere reasonably free from dust.

A clean glass tray is preheated in a stream of warm water adjusted to about 32° C. A freshly filtered portion of developing solution D-19 of sufficient volume to cover the plate is likewise warmed to 32° C. Remove the plate from contact camera, place in a tray, cover with developer solution and rock the dish for two minutes. Pour off developer and discard, introduce about 100 ml. of distilled water at 25° C., directing the stream against the walls of tray and discard after rinsing plate for about 30 seconds. Treat the plate with about 50 ml. of Eastman Tropical Hardener SB-4 keeping the tray in motion for about one minute and then continuing the hardening process for another two minutes with solution remaining quiescent. Discard hardening solution and introduce about 50 ml. of freshly filtered fixing solution, formula F-5. Complete solution of the silver halides is usually effected in 15 minutes; longer periods of fixation do not harm the emulsion. Wash the plate in a stream of filtered tap water for about two hours.

RESOLVING POWER OF ALPHA RAY PATTERN

The radiographic image developed on the fine grain alpha particle plate is sharply defined and is capable of considerable magnification. Examination of Fig. 5 shows that only those radioactive nuclei located on the polished surface and the immediate thin layer defined by the range in the mineral of the most penetrating alpha ray will register an image on the emulsion. Grains of uranium and thorium minerals as small as 20 microns diameter are readily detected when embedded in a

non-radioactive matrix by examining the pattern by transmitted light at a magnification of 100 diameters. These minute grains are readily differentiated by a surrounding halo of alpha particle tracks from opaque dust specks that occasionally contaminate the processed emulsion. The pattern provided by a radioactive grain of finite dimensions consists

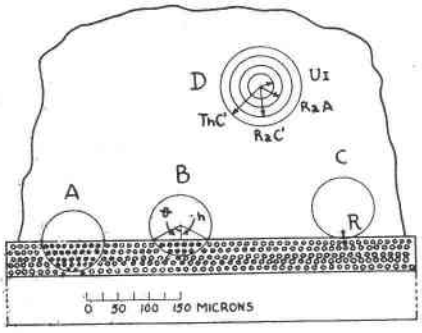

FIG. 5. Diagrammatic representation of action of alpha rays on emulsions desensitized to beta and gamma radiations.

Radii of circles about point *D* represent relative ranges of different alpha rays which may be ejected from any point in the mineral. The radii of circles, *A*, *B* and *C* represent the range of the most penetrating ray at different levels above the polished surface. In the illustration the permeability to alpha rays is the same for both the mineral and the emulsion. A latent image is produced wherever rays penetrate the emulsion.

of a series of alpha particle tracks, the greater number of which are oriented at right angles to the emulsion layer. A small fraction of the alpha rays, originating from nuclei near the extreme edges of the grain, strike the emulsion laterally and their trajectories are recorded by the emulsion as individually resolvable tracks.

Measurements by Wilkins (92) of the range of alpha particles in silver halide gelatin emulsions show that the stopping power of the recording medium is 1300 times as great as that of air. Alpha rays emitted by RaC′ and ThC′ will therefore have a range in the emulsion of 53 and 66 microns, respectively. A point source of alpha ray activity in direct contact with the plate will generate a hemisphere of individual tracks in the emulsion which may attain a maximum radius of 66 microns. Since the emulsion is observed in a plane at right angles to the optic axis of the microscope, only the horizontal projection of the tracks is observed. In general, the visual annulus of diffusion about the image of the grain is less than the maximum range of the most penetrating alpha particle. The horizontal projection of rays impinging into the emulsion at the median angle of 45° is equal to $R/\sqrt{2}$, which is equal to 38 and 47 microns

for alpha particles ejected from RaC′ and ThC′, respectively.

Comparative microscopic measurements of the dimensions of mineral grains on the polished surface and their corresponding alpha ray patterns show that the width of the diffuse annulus varies between 30 and 40 microns. A sample of calcite from Joachimsthal, Bohemia, containing minute inclusions of pitchblende, proved a serviceable test specimen for measuring the diffuseness in the image caused by the lateral alpha rays.

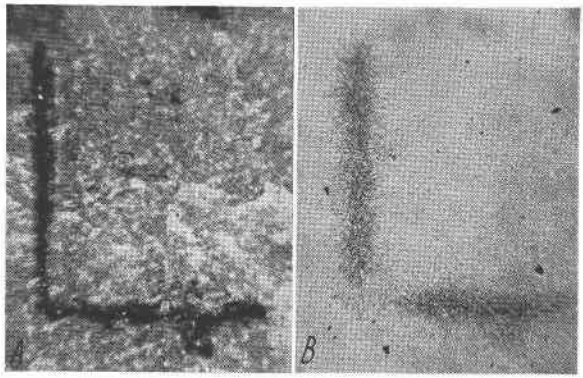

FIG. 6. Resolving power of alpha ray pattern.

Comparative photomicrographs at 100× (reduced ½ in reproduction) of a pitchblende inclusion in a non-radioactive matrix. Sample collected by Charles R. Toothaker at Joachimsthal, Bohemia.

(*A*) Polished section under oblique illumination.

(*B*) Alpha ray pattern under transmitted axial illumination.

Figure 6 reproduces one of the minute radioactive inclusions, *A*, and its corresponding alpha ray pattern, *B*, at 100 diameters magnification. The width of the angular inclusion measures 10 microns; at the same point, the radiographic image averages 70 microns. This corresponds to a lateral alpha ray diffusion of 30 microns on each side of the image proper, in close agreement with the theoretical deductions. This factor also causes an apparent diminution in the dimensions of non-radioactive inclusions in matrices of uranium and thorium bearing minerals which must be taken into consideration when the foreign bodies are very minute. Thus, a gangue vein less than 60 microns wide may appear to be feebly radioactive as a result of scattered alpha rays from the surrounding matrix.

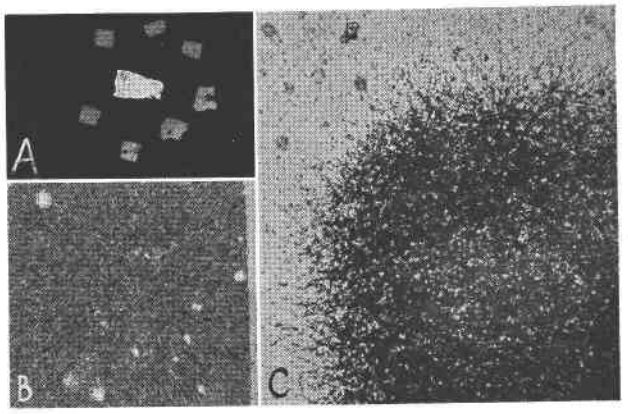

FIG. 7. Successive stages in the magnification of an alpha ray pattern.

(*A*) Group of thorianite crystals from Bambaraluma Valley, Ceylon (U. S. National Museum no. 94346) surrounding a central chip of uraninite from Katanga, Belgium Congo. Full sized positive print from pattern.

(*B*) Photomicrograph at 20× of alpha ray pattern of an entire crystal showing non-radioactive inclusions.

(*C*) Corner of thorianite cube at 200× (reduced $\frac{1}{3}$ in reproduction) showing some alpha ray tracks which struck the emulsion at glancing incidence.

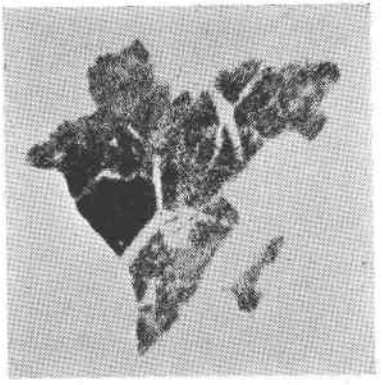

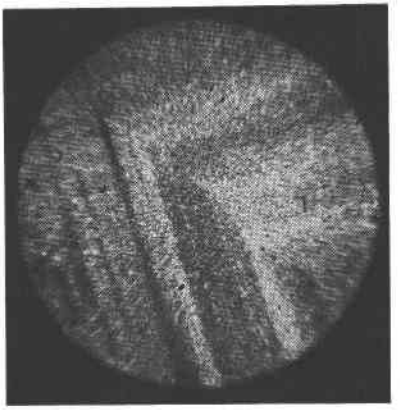

FIG. 8

FIG. 9

FIG. 8. Photomicrograph at 20× (reduced $\frac{1}{3}$ in reproduction) from alpha ray pattern of an altered thorianite. Sample collected by A. Rosenzweig at Easton, Pa.

FIG. 9. Alpha ray pattern, enlarged 15× (reduced $\frac{1}{3}$ in reproduction) of section of samarskite from Mitchell Co., N. C. Sample no. 1849 of Brush Mineral Collection.

Although it has these limitations, the alpha ray pattern is still capable of yielding images of radioactive minerals which provide serviceable information concerning the relative concentration and distribution of alpha ray activity on successive magnification up to about 200 diameters. Figure 7 (*A*) reproduces the alpha ray pattern of a group of thorianite crystals which, considered as a macro print, shows the uniform distribution of uranium and thorium in the crystals, and that their alpha ray activity is less than the central chip of uraninite. A photomicrograph of one of the crystals at 20× magnification, Fig. 7 (*B*), shows the presence of minute non-radioactive inclusions. Further magnification of a corner of the alpha ray pattern reveals the scattered alpha ray tracks ejected from the edges of the cubic crystal. In contrast to the uniform distribution of uranium and thorium in the Ceylon thorianite, an alpha ray pattern of thorianite from Easton, Pa., Fig. 8, shows a considerable variation in alpha ray activity corresponding to graded zones of alteration evident on examination of the polished section.

The excellent resolving power of the fine grain alpha ray emulsion[6] permits the sharp delineation of variations in the spatial distribution of uranium and thorium along the crystallographic axes of crystals that appear to be optically homogeneous. A striking example of this varied deposition is furnished by an alpha ray pattern, Fig. 9, of a mounted section of samarskite. Assuming a linear proportionality between the alpha ray activity and photographic density in the image, a variation of 3 per cent uranium (and thorium) is exhibited between the zones of maximum and minimum blackening. This phenomenon is recorded vaguely on light sensitive photographic plates and only idealized sketches from such autoradiographs have been capable of reproduction in the past (25).

Classification of Uranium and Thorium Minerals According to Alpha-Ray Activity

Radiometric methods of analysis have been applied in the classification of radioactive minerals. By comparing the activity of the powdered mineral and a similar layer of uranium oxide Goldschmidt (28), employing a gold leaf electroscope, observed an approximately linear relationship between the measured activity and the theoretical alpha ray activity that can be calculated from the uranium and thorium content with the

[6] According to Mees (59) the resolving power of photographic plates for optical images ranges between 18 to 30 microns depending upon the speed of the emulsion. The resolution of this contact process is of the same order of magnitude.

aid of the rule[7] formulated by McCoy and Ross (58). The blackening produced on a photographic plate is also a measure of the relative radioactivity and this lends itself to the identification of radioactive inclusions. The variation in photographic density is sufficiently marked, even in the case of emulsions responding to beta radiations, so that minerals in which uranium and thorium are principal components can be differentiated readily from species in which these elements occur only as minor constituents. As a type example of such application may be cited the identification by Goddard and Glass (27) of grains of uraninite in a feebly radioactive cerite. Since the emulsion under consideration is a highly selective recording medium for alpha particles, investigations were conducted to test its suitability as a quantitative tool for recording the number of alpha particles escaping from a polished surface of a radioactive mineral.

The photographic density of the alpha ray pattern is a measure of the number of particles which entered the emulsion during the period of exposure. For mineral species sufficiently old for the attainment of radioactive equilibrium, the number of alpha particles escaping through the polished surface is proportional to the uranium and thorium content and provides a convenient index for the analytical grouping of the radioactive minerals. Unlike the complex ionization produced by an alpha particle at different points of its range through air,[8] the photographic action on silver halide grains is uniform throughout the path of the alpha ray and the photographic density is directly proportional to its range in the emulsion (44). Hence, an approximately linear function is to be expected between the photographic density, D = log (incident light/transmitted light) of an alpha ray pattern and the number of particles striking a unit area of the emulsion per unit of time, P_α.

The exact evaluation of the number of alpha particles producing the blackening is a problem of considerable difficulty owing both to the variation in range of rays produced by the numerous members of the uranium, actinium and thorium series and to the loss of part of their

[7] When the unit of activity is that due to 1 sq. cm. of a thick film of U_3O_8, then the radioactivity, as measured by the electroscope, of any mineral which is sufficiently old for the establishment of radioactive equilibrium is expressed by 3280U+953Th, where the respective symbols refer to the weight of uranium and thorium present in 1 gram of the mineral.

[8] The early work of McCoy and Leman (56) on the ionization produced by alpha rays showed that the number of ion pairs generated by the passage of an alpha ray through air is proportional to the $\frac{2}{3}$ power of its range, The more recent treatment of the problem by Evans (22) and Goodman and Evans (23) shows that the total ionization above a thick solid emitting alpha particles is only approximated by the $\frac{2}{3}$ power rule in the limiting case of very long range rays.

energy in traversing the mineral before they strike the emulsion. An approximate solution is secured by assuming that the ejection of all particles from a given point is equally probable and that the disintegration of each series can be represented by a single hypothetical particle having a range, $\overline{R}_U$, $\overline{R}_{Th}$, which is equal to the arithmetical mean of the ranges of the several members of the uranium and thorium series, as expressed by equations (2) and (3)

(2) $\overline{R}_U = [R_{U_I} + R_{U_{II}} + R_{I_0} + R_{Ra} + R_{Rn} + R_{RaA} + R_{RaC'} + R_{RaF}]/8 = 4.04$ air cm.

(3) $\overline{R}_{Th} = [R_{Th} + R_{RdTh} + R_{ThX} + R_{Tn} + R_{ThA} + R_{ThC'}]/6 = 5.11$ air cm.

According to the measurements of Rutherford and Geiger (75) the total number of alpha particles emitted by a mineral containing 1 gram of uranium in equilibrium with its disintegration products is 9.67×10^4 per sec.[9] The corresponding number emitted by 1 gram of thorium in equilibrium with its disintegration products is $0.36 \times 9.67 \times 10^4 = 3.48 \times 10^4$ per sec. The number of alpha particles generated, N_g, in a thin slab of mineral of density ρ defined by 1 sq. cm. of the polished surface and the range of the average alpha rays is then expressed by the summation of equations (4) and (5) in which the symbols U and Th represent the weight of uranium and thorium per gram of mineral.

(4) $$N_g^U = \overline{R}_U \rho U \times 9.67 \times 10^4$$

(5) $$N_g^{Th} = \overline{R}_{Th} \rho Th \times 3.48 \times 10^4$$

Substituting expression (1) for the range[10] of an alpha particle in a solid, yields:

[9] This value includes the number of alpha particles formed during the disintegration of the actinium series. The studies of von Grosse (89) show that the activity ratio of actinium to the uranium-radium series is 4:100. In view of the small number of actinium alpha rays generated in the thin section, but little error is introduced by assigning the same value for the average range of the hypothetical alpha particle to both the uranium and actinium series.

[10] The range as calculated from the Bragg-Kleeman rule must be considered only as a rough approximation when dealing with the complex minerals represented by the multiple oxides. Specimens like samarskite contain as many as 36 individual atomic species (counting all members of the rare earth group), and though the rule yields values in close agreement with experimental measurements in the case of elementary metals and relatively simple mixtures of gases, it is problematical whether it is equally applicable to the more complex uranium and thorium minerals. In evaluating the permeability by means of equation (1) minor constituents of low atomic weight were not tallied individually to simplify the labor of computation. Their contribution to the stopping power is relatively minute and their elimination causes only a small increase in the atomic oxygen count which is obtained by difference after the major atomic units are computed.

$$N_g^U = \psi U \left(0.00215 \times \frac{4.04}{6.97}\right) 9.67 \times 10^4 = 120.5\psi U \tag{6}$$

$$N_g^{Th} = \psi Th \left(0.00215 \times \frac{5.11}{6.97}\right) 3.48 \times 10^4 = 54.8\psi Th \tag{7}$$

$$N_g = N_g^U + N_g^{Th} = \psi(120.5U + 54.6Th). \tag{8}$$

Only a small fraction of the alpha particles generated in the effective thin section are capable of striking the emulsion. The particles are ejected at random and statistically one-half the number generated will be directed away from the emulsion. Study of grain *B* in Fig. 5 reveals that of the remaining number headed towards the emulsion only those rays subtended by the solid angle formed by the rotation of 2θ will be capable of reaching the polished surface. A formal mathematical treatment of the number of alpha particles escaping through a solid surface by Evans (22) shows that only one-fourth of all alpha rays generated will escape through the polished surface. Hence, the photographic density of the image may be expected to be proportionate to a value P_α representing the number of alpha particles which escape per second from 1 sq. cm. of polished mineral surface.

$$P_\alpha = N_g/4 = \psi(30.1U + 13.7Th) \tag{9}$$

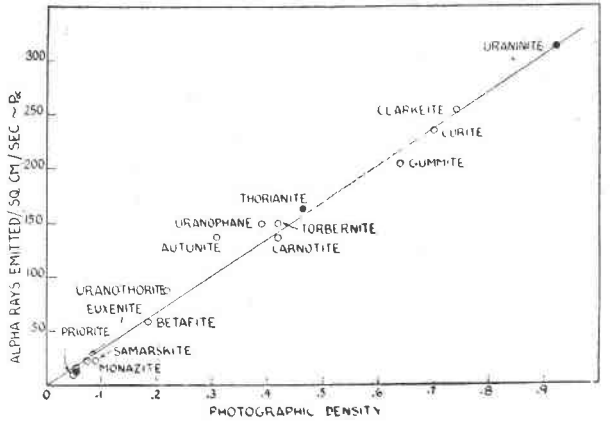

FIG. 10. Graph showing the relationship between the photographic density of the pattern and the number of alpha rays striking the emulsion.

To test the validity of this equation, a series of polished sections containing homogeneous chips of minerals of varying uranium and thorium content was exposed against a fine grain alpha particle emulsion for 115 hours and the photographic density of the developed images were measured by means of a recording microdensitometer. The results of this

experiment are plotted in Fig. 10. Using the same specimens, exposure time, and conditions of development, repeated experiments showed that the densities of the images are reproducible on different plates within an error of 1 per cent when the photographic density is about 1.0, and about 10 per cent for faint images (D = 0.1). The solid circles ● represent minerals whose uranium and thorium content was determined by the author on portions of the specimen adjoining the material from which the polished sections were prepared. The P_α values assigned to these minerals, uraninite 313, thorianite 164, and monazite 14.2 probably correspond closely to the alpha ray activity exhibited by the corresponding polished sections. Points ⊙ represent minerals whose P_α value was computed from analyses recorded in the literature on specimens from the same locality as the chips selected for study. These values are not as reliable as those based on direct analysis, as the chips studied may not in all cases be representative of the material originally selected for analysis. In general, the curve shows a direct proportionality between the photographic density of the image and the alpha ray activity computed from equation (9) over a wide range of uranium and thorium contents. The departure from exact linearity is well within the range of uncertainty in the evaluation of P_α and the measurement of the photographic density. A contributory factor in the more marked deviations of autunite (23.9 per cent), uranophane (8.7 per cent), and uranothorite (17 per cent) is the non-attainment of radioactive equilibrium. Studies by Gleditsch on Norwegian uranothorites show that the ratio of radium to uranium in this mineral is usually lower than the equilibrium amount (26).

The linear relationship[11] between the photographic density and the alpha ray activity of the polished surface permits the classification of the uranium and thorium minerals in accordance with their relative P_α values and presents a simple means for their qualitative grouping as an

[11] The data presented in Fig. 10 do not prove the absolute validity of the coefficients in eq. (9) as these are based on a series of simplifying assumptions. In order to check these calculated values, the number of alpha particles escaping from the polished surface was counted by observing the scintillations on a zinc sulfide screen placed over a fixed area of the mineral. These counts were considerably lower than the P_α calculated for the mineral. The observed count was about 15 per cent of the theoretical for uranium minerals, and about 25 per cent for minerals whose activity was due chiefly to thorium isotopes. The direct counting of scintillations is very difficult, particularly for an observer with little experience in the technique, and the eye is probably able to detect only the brilliant flashes caused by the more energetic RaC′ and ThC′ rays, so that the more abundant short ranged particles escape detection. This is confirmed by the higher count on thorium minerals whose alpha rays are more energetic than those produced in the uranium series. The uncertainty in the absolute values of P_α does not invalidate the proposed classification as any change in the value of the coefficients will be consistent for all minerals in the tabulation.

aid for their identification. The known uranium and thorium minerals can be segregated into seven groups on the basis of their relative alpha ray activity. The members of these groups are listed in Table 3 in the order of their average P_α values as computed from their chemical composition.[12] The variation of uranium and thorium contents within a mineral species is in several cases sufficiently wide to cause overlapping into more than one group; such minerals are listed under both groupings. A considerable number of the minerals listed represents species of very rare occurrence and the evaluation of the P_α value is based only on a single analysis of the material from the type locality.

In practice, the mounted specimen is surrounded by an annulus, Fig. 4, in which are embedded chips of known minerals whose P_α is representative of the group. The two units are exposed simultaneously for 100 hours and the developed plate is examined in a uniform field of transmitted light. Interposing an opal glass between the plate and the light source facilitates the observation of very weak images. Under these conditions of illumination, 20 per cent variations in photographic density are easily discernible. The intensity of radioactive inclusions revealed by the pattern is compared visually with the surrounding images produced by the standard chips and a group number is assigned to the unknown constituents. In making such visual comparisons the images should be masked so that nearly equal areas of the standard and unknown patterns are exposed to view in order to avoid fallacious interpretations of density due to marked inequality in the size of the patterns. When the density falls on the borderline of two standards, the grouping of greater alpha ray activity should be assigned in order to compensate for the small loss of radon or thoron incurred during the mounting and polishing of the specimen. A plate of this character, showing a polished section containing radioactive inclusions and the surrounding alpha ray patterns of the standards, is reproduced in Fig. 11. Minerals belonging to group *G* have a very low uranium and thorium content and do not produce a discernible image after 100 hours exposure. If such species are suspected from the behavior of the massive material towards an electroscope or a Geiger counter, the polished section must be exposed from 250 to 1000 hours in order to secure an image of suitable density for the localization of the individual radioactive grains.

[12] The analyses of the minerals investigated were selected chiefly from the tabulations in Dana's "System of Mineralogy" (15, 70), Doelter's "Handbuch der Mineralchemie" (19) and the analytical data listed by Holmes (38) in his studies on the age of the earth. Table 3 also includes all new species and varieties of uranium and thorium minerals that have been described since 1931, the date of the last comprehensive listing of the radioactive minerals (38).

The tabulation does not include minerals which only occasionally occur with appreciable amounts of uranium. Among these may be mentioned a garnet-like mineral from Argentina (38) carrying 0.4 per cent U_3O_8 and an iron-lime garnet from Hybla, Ontario, found by Ellsworth (21) to exhibit a weak radioactivity. Ellsworth also describes two alteration products of thorite, a white mineral alpha-hyblite and a yellow brown variety,

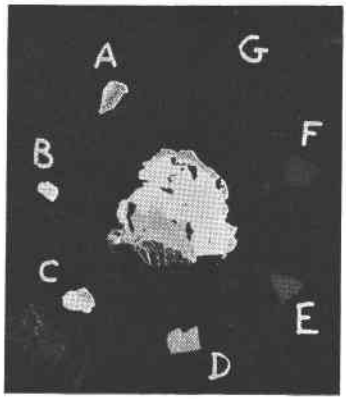

FIG. 11. Positive print from alpha ray pattern of a uranium ore and surrounding radioactive mineral standards.

(*A*) uraninite; (*B*) thorianite; (*C*) torbernite; (*D*) uranothorite; (*E*) samarskite; (*F*) monazite; (*G*) microlite.

The contrast on the alpha ray plate is greater than that exhibited in positive print reproduction.

beta-hyblite, which appear to be hydrous, basic sulphosilicates of thorium. Lack of analytical data prevents the listing of davidite which appears to be a mixture of several minerals and whose radioactivity may be due to the carnotite observed to be present (70). Northrop (67) lists an unnamed thorium mineral from Harding Mine district, New Mexico, with 32.35 per cent thorium and 0.185 per cent uranium which is probably a member of group *E*. The unnamed multiple oxides of ZrO_2-TiO_2-ThO_2 descbried by Blake and Smith (70, p. 741) have a computed P_α of 23–28 for the thorian members.

This method of classification is applicable whenever the mineral is sufficiently old for the attainment of radioactive equilibrium. This condition is attained when the age of the mineral exceeds 1,000,000 years. However, if an overall error of 10 per cent is allowed in the estimation of P_α and the measurement of the photographic density then minerals only 250,000 years old will produce sufficient alpha radiation necessary for the production of an image whose density approximates that stipu-

lated by equation (9). In a study of about 200 polished samples of uranium and thorium minerals, representing 41 species, only two specimens were observed for which the density of the alpha ray image differed radically from the theoretical alpha ray activity, P_α. Coatings of autunite on feldspar, from Spruce Pine, N. C., failed to give an alpha ray pattern after an exposure of 500 hours.[13] The other exception is thorotungstite (78), which failed to produce an image after 1000 hours' exposure. Both minerals are probably of very recent origin.

Another factor which must be considered in the evaluation of the alpha ray pattern is the possibility that in the preparation of the section the cutting wheel intersected the mineral grain at an extreme edge, leaving a thickness of material behind the exposed face less than the range of the most penetrating alpha ray in the mineral. Under these circumstances, which become more probable the smaller the grain size of the inclusions, the image will be less intense than that stipulated by theory. It is noteworthy that P_α is a rather unusual physical property, embodying extensive as well as intensive functions. The P_α remains constant and is independent of the thickness of the specimen provided it exceeds a minimum thickness of about 30–60 microns. When the grain size falls below this limiting thickness, P_α no longer characterizes the mineral. This difficulty is encountered when very fine grains are dispersed uniformly in an inert matrix. Thus, most analyses of pure pitchblende lead to a P_α value of 278–246. The crude ore, however, may contain about 30 per cent silica or clay which dilutes the alpha ray activity per unit area and results in an image of lower photographic density. Occurrences of pitchblende in which the grain size of the pure mineral is smaller than the critical grain size are allocated to groups *B* and *C*.

Alteration and the partial leaching of radium will give rise to variation in alpha ray activity of the resultant mineral. Such conditions have been described by Lind (53) in the sampling of carnotite ores for electroscopic assay; and the presence of radium in excess of the amount in radioactive equilibrium with uranium has been demonstrated by Kurbatov (46) in different portions of tyuyamunite. The leaching of radium from a primary mineral and its redeposition along the outer border of the alteration product is frequently observed in nodules of gummite (Fig. 12). The exposed radium is brought into solution by percolating waters and may again be deposited when the solution comes in contact with lead or barium minerals capable of adsorbing radium sulfate. This phenomenon gives rise to minerals with an alpha ray activity in the absence of uranium

[13] Massive samples of the mineral from Autum, France, and Mt. Painter, S. Australia, furnished an alpha ray pattern of density proportional to the P_α range of autunite.

or thorium. A radioactive pyromorphite from Isay l' Eveque, France, has been reported by Danne (16) and the activity was shown to be a surface adsorption phenomenon by McCoy (57). Another sample of pyromorphite from Gennammari, Sardinia, has been described by Misciatelli (62) as having an activity equivalent to 0.0028 grams of U_3O_8 with chemically detectable amounts of uranium or thorium absent. Likewise, radioactive barite from Carlsbad in which the activity is derived from adsorbed radium have been analyzed by Haberlandt (33).

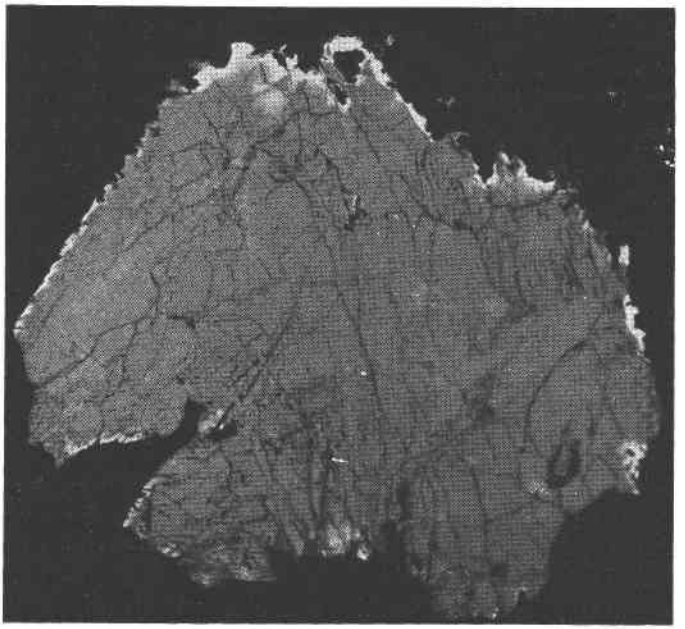

FIG. 12. Alpha ray pattern, enlarged 7× (reduced ½ in reproduction) of complete cross-section of a gummite nodule. Sample collected at the English Knob Mine, Spruce Pine, N. C., by F. A. Lewis. The white areas correspond to regions of high alpha ray activity.

Interference by Samarium: As noted in the introduction, Sm^{148} emits alpha rays, and its potential interference must be considered as it is present in those uranium and thorium minerals that contain the rare earth oxides. The element emits 150 alpha rays per sec. per gram having a range of 1.28 cm. in air (23). In a mineral containing little uranium and thorium and about 10 per cent samarium, there is a possibility that the activity of the samarium contributes appreciably to the density of the alpha ray pattern. Calculations based on the permeability of allanite to the alpha particle emitted by samarium show that the number of rays

A

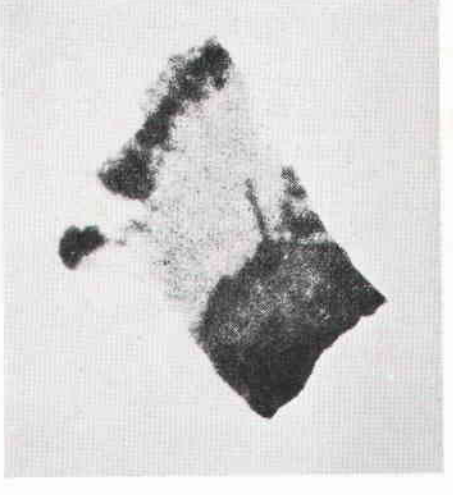

B

FIG. 13. Plates, showing variation in alpha ray activity of secondary uranium minerals from the Katanga, Belgium Congo deposits.

(*A*) Polished section, oblique illumination, 10×. Uppermost layer, curite; center, torbernite; bottom, gummite.

(*B*) Alpha ray pattern, axial illumination, 10×.

contributed is only 0.009 per sq. cm. per sec., whereas the P_α due to uranium and thorium present ranges between 1 and 2.6. With increase in the P_α value of the mineral the contribution of the samarium alpha rays becomes entirely negligible. The samarium contributes about 0.5 per cent to the alpha ray pattern of allanite, 0.05 per cent to that of samarskite and only 0.001 per cent to that of cleveite.

These are of rare occurrence and for most samples the classification has proven of utility as a first step towards the identification of radioactive inclusions. The variation in alpha ray activity corresponding to different mineral species occurring in close association is illustrated by the complex alteration products of uraninite characteristic of the Belgian Congo deposits, a study of which is presented in Fig. 13. At the present writing, mineralographic description of opaque uranium and thorium minerals is entirely lacking except for a brief description of uraninite by Schneiderhöhn (77) and Short (80). The petrographer must therefore adapt the descriptions available in the literature for massive material to interpretation of microscopic observations, or preferably compare the surface under study with polished sections of known material. It is difficult to obtain authentic samples of the less common species. Optical data for the better defined uranium and thorium minerals are recorded by Larsen and Berman (49).

Work is in progress directed towards the further identification of the radioactive mineral species by means of hardness tests, color of the micro streak,[14] fluorescence under ultraviolet light, and the localization of constituent metals and radical groupings by chemical printing techniques (96).

Summary

The complex group of uranium and thorium minerals is characterized by the production of a selective alpha ray pattern on a photographic emulsion desensitized to light. The relative intensity of the image permits the subdivision of the radioactive minerals into a series of seven groups as a preliminary step towards their identification in polished section. The emulsion has been studied intensively with respect to its behavior towards electromagnetic radiations, and pseudophotographic agents, and

[14] It has been found practical to study the nature of the streak produced on polished surfaces by transferring the powder from the scratch mark onto moist gelatin paper and examining the physical replica under oblique illumination. Preliminary experiments show that the minute streak exhibits the same characteristics as the macro streak on porcelain and individual grains can be tested microscopically by means of solvents and reagents. Details of this technique will be published shortly.

a suitable developing procedure has been devised for the production of a sharply defined autoradiographic image of reproducible density. The emulsion exhibits marked fading of the latent image on delayed development and the latent image is completely destroyed by exposure to mercury vapor.

ACKNOWLEDGMENTS

The author wishes to express his appreciation to E. P. Henderson of the U. S. National Museum for his cooperation in providing samples of radioactive minerals employed in these studies. Thanks are also due to George Switzer, curator of the Brush mineral collection at Yale University, for providing chips of the less common uranium and thorium minerals for use in the preparation of polished sections. The services of Mardalee Bishop in checking the numerous calculations of the permeability and alpha ray activity values are gratefully acknowledged. The writer is particularly indebted to William C. White for numerous measurements of photographic density on a recording microdensitometer. The writer expresses his appreciation to H. L. Andrews for critical reading of the manuscript. Of equal importance in the pursuit of these studies is the encouragement received from Medical Director Paul A. Neal, Chief, Industrial Hygiene Research Laboratory, while the work was in progress.

TABLE 3. CLASSIFICATION OF THE URANIUM AND THORIUM MINERALS
(The more common species are indicated in bold faced type)

GROUP A: $P_\alpha = 338-224$

Uraninite: crystalline UO_2+UO_3 and minor ThO_2.
Bröggerite: thorian uraninite.
Cleveite, Nivenite: yttrian and cerian uraninites.
Pitchblende: massive U_3O_8 with traces of ThO_2 and rare earth oxides.
Clarkeite: sodian gummite.
Becquerelite: $2UO_3 \cdot 3H_2O$.
Curite: $2PbO \cdot 5UO_3 \cdot 4H_2O$.
Schoepite: $4UO_3 \cdot 9H_2O$.
Ianthinite: $2UO_2 \cdot 7H_2O$.
Soddyite: $12UO_3 \cdot 5SiO_2 \cdot 14H_2O$.
Rutherfordine: $UO_2 \cdot CO_3$.
Sharpite (61): $6UO_3 \cdot 5CO_2 \cdot 8H_2O$.

GROUP B: $P_\alpha = 223-149$

Fourmarierite: $PbO \cdot 4UO_3 \cdot 5H_2O$.
Phosphuranylite: $3UO_3 \cdot P_2O_5 \cdot 6H_2O$.
Gummite: $UO_3 \cdot nH_2O$.
Vandenbrandite: $CuO \cdot UO_3 \cdot 2H_2O$.
Zippeite: $2UO_3 \cdot SO_3 \cdot 4H_2O$.

Voglianite, Uraconite, Medjidite, Uranopilite[15] } sulfates of uranium of uncertain composition.

Thorianite[16]: essentially ThO_2 with minor UO_2+UO_3.

Renardite, Dumontite, Dewindtite, Stasite } lead uranyl phosphates of uncertain composition.

Trögerite: $3UO_3 \cdot As_2O_5 \cdot 12H_2O$.
Sklodowskite: $MgO \cdot 2UO_3 \cdot 2SiO_2 \cdot 6H_2O$.
Cuprosklodowskite (88): $CuO \cdot 2UO_3 \cdot 2SiO_2 \cdot 6H_2O$.
Uranosphaerite: $Bi_2O_3 \cdot 2UO_3 \cdot 3H_2O$.
Saléite (86): $MgO \cdot 2UO_3 \cdot P_2O_5 \cdot 8H_2O$.
Pitchblende, dispersion of U_3O_8 in silica or clay.

GROUP C: $P_\alpha = 148–100$

Uranocircite: $BaO \cdot 2UO_3 \cdot P_2O_5 \cdot 8H_2O$.
Thorogummite: an alteration product of thorianite.
Nicolayite (82): similar to thorogummite.
Yttrogummite: an alteration product of cleveite.
Uranospinite: $CaO \cdot 2UO_3 \cdot As_2O_5 \cdot 8H_2O$.
Zeunerite: $CuO \cdot 2UO_3 \cdot As_2O_5 \cdot 8H_2O$.
Torbernite: $CuO \cdot 2UO_3 \cdot P_2O_5 \cdot 8H_2O$.
Johannite: $(Cu,Fe,Na_2)O \cdot UO_3 \cdot SO_3 \cdot 4H_2O$.
Autunite: $CaO \cdot 2UO_3 \cdot P_2O_5 \cdot 8H_2O$.
Bassetite[17]: $FeO \cdot 2UO_3 \cdot P_2O_5 \cdot nH_2O$.
Fritzscheite: $MnO \cdot 2UO_3 \cdot P_2O_5 \cdot nH_2O$.
Kasolite: $3PbO \cdot 3UO_3 \cdot 3SiO_2 \cdot 4H_2O$.
Uranophane: $CaO \cdot 2UO_3 \cdot 2SiO_2 \cdot 6H_2O$.
Carnotite: a hydrous vanadate of uranium and potassium.
Tyuyamunite: a hydrous vanadate of uranium and calcium.
Mackintoshite: a hydrous silicate of thorium and uranium.
Maitlandite (82): a variety of mackintoshite.
Brannerite: a hydrous titanate of uranium and rare earth oxides.
Crude Pitchblende: dispersions of U_3O_8 in siliceous rocks.

GROUP D: $P_\alpha = 99–50$

Uranothorite: a hydrous silicate of thorium and uranium.
Orangite: a variety of uranothorite.
Enalite (43): a variety of uranothorite.
Auerlite: phosphorian thorite.
Hydrothorite: essentially $ThSiO_4 \cdot 4H_2O$.

[15] Nováček (68) describes a bright yellow uranopilite, $6UO_3 \cdot SO_3 \cdot 16–17H_2O$ which changes on partial dehydration to a grayish-brown beta-uranopilite, $6UO_3 \cdot SO_3 \cdot 10H_2O$.

[16] Bespalov (7) describes a new variety of thorianite with 11.2–12.5 per cent lead.

[17] Bassetite originally described as a variety of autunite has since been shown by Meixner (60) to be a distinct species differentiated from autunite by its lack of fluorescence in ultraviolet light and the presence of iron in place of calcium.

Ferrothorite (48,83): ferrian thorite.
Calciothorite: calcian thorite.
Parsonite: a lead uranyl phosphate.
Uranothallite: $2CaO \cdot UO_2 \cdot 4CO_2 \cdot 10H_2O$.
Uranochalcite: a hydrous sulphate of uranium with variable amounts of copper and calcium.
Volgite: possibly a cuprian uranothallite.
Randite: a hydrous carbonate of calcium and uranium.
Uvanite: $2UO_3 \cdot 3V_2O_5 \cdot 15H_2O$.
Walpurgite: $5Bi_2O_3 \cdot 3UO_3 \cdot 2As_2O_5 \cdot 12H_2O$.
Betafite: a multiple oxide of uranium, columbium and tantalum.
Samiresite: plumbian betafite.
Blomstrandite: titanian betafite.
Mendeleyevite: calcian betafite
Ishikawaite: a multiple oxide of uranium, columbium, tantalum and rare earths.
Schroeckingerite[18]: $3CaCO_3 \cdot Na_2SO_4 \cdot UO_3 \cdot 10H_2O$.

GROUP E: $P_\alpha = 49-16$

Thorite: a thorium silicate, with uranium less than 2 per cent.
Eucrasite: cerian thorite.
Ellsworthite: uranian pyrochlore.
Hatchettolite: uranian pyrochlore.
Rauvite (76): $CaO \cdot 2UO_3 \cdot 6V_2O_5 \cdot 20H_2O$.
Ampangabeite: multiple oxide of columbium, rare earths and uranium.
Pisekite: possibly a variety of ampangabeite.
Freyalite: cerian thorite.
Djalmaite: possibly a tantalian variety of betafite.
Samarskite: a complex multiple oxide of uranium, rare earths, columbium and tantalum.
Nohlite: variety of samarskite.
Plumboniobite: plumbian samarskite.
Calciosamarskite: calcian samarskite.
Euxenite: a multiple oxide of columbium, titanium and rare earths.
Toddite: a variety of euxenite.
Polycrase: titanian member of euxenite–polycrase series.
Khlopinite: variety of euxenite–polycrase.
Fergusonite: essentially a multiple oxide of yttrian earths, columbium and tantalum.
Bragite: uranian fergusonite.
Vietinghofite: ferroan samarskite.
Delorenzite: a stanniferous multiple oxide of titanium, rare earths and uranium.
Thorotungstite (78): $2WO_3 \cdot 2H_2O + (ThO_2, Ce_2O_3, ZrO_2) \cdot H_2O$.

GROUP F: $P_\alpha = 16-5$

Cyrtolite, uranian (64): a hydrous silicate of zirconium.
Priorite, thorian: a multiple oxide of columbium, tantalum, yttrian earths and thorium.
Eschynite: a multiple oxide of columbium, tantalum, cerian earths and thorium.
Yttrialite: a silicate of yttrian earths and thorium.
Yttrocrasite: a multiple oxide of yttrian earths and titanium.

[18] The mineral dakeite described by Larsen and Gonyer (50), has been shown to be identical with schroeckingerite by Nováček (69).

Caryocerite: a complex silicate of thorium and rare earth oxides.
Yttrotantalite: a multiple oxide of yttrian earths, columbium and tantalum.
Yttrocolumbite (52): probably identical with yttrotantalite.
Hjelmite: a stanniferous multiple oxide of rare earths, columbium and tantalum.
Monazite[19]**:** phosphate of cerian earths and thorium.
Tritomite: a rare earth fluo-boro-silicate.
Tanteuxenite: tantalian euxenite.
Naëgite: a variety of zircon containing columbium and rare earth oxides.
Zirkelite: a multiple oxide of zirconium, titanium and thorium.
Thucholite[20]: a thorian hydrocarbon.
Microlite: tantalian member of pyrochlore-microlite series.
Pyrochlore: columbian member of pyrochlore-microlite series.
Fergusonite: a multiple oxide of yttrian earths, columbium and tantalum.
Risörite: titanian fergusonite.
Sipylite: yttrian fergusonite.
Kochelite: an altered fergusonite.
Rutherfordite: an altered fergusonite.
Yamagutilite (42): variety of zircon containing rare earths, uranium and thorium.
Lyndochite: a thorian and calcian variety of euxenite-polycrase.
Steenstrupine: a hydrous thorian rare earth silicate.
Xenotime: phosphate of yttrian earths.

GROUP G: $P_\alpha = 4-0$

Microlite: varieties containing only traces or no uranium and thorium.
Eschwegite: probably a variety of euxenite.
Homilite (38): borosilicate of calcium and iron.
Erdmannite: a variety of homilite of uncertain composition.
Cyrtolite: an altered zircon with traces of uranium.
Corvusite: a hydrous oxide of vanadium with associated traces of uranium.
Priorite: a multiple oxide of yttrian earths, columbium and tantalum.
Wiikite: a multiple oxide of columbium, tantalum, titanium and rare earths.
Nuolaite: a thorian variety of wiikite.
Asphaltite (17): a uranian hydrocarbon.
Erikite: a silicophosphate of rare earths and aluminum.
Nagatelite (39): composition similar to erikite and possibly identical with it.
Melanocerite: a fluosilicate of rare earth oxides.
Allanite: a cerian epidote.
Polymignyte: a multiple oxide of zirconium, titanium, columbium and tantalum.
Zircon: $ZrO_2 \cdot SiO_2$.
Hagatalite (41): possibly a columbian-tantalian variety of zircon.
Oyamalite (41): variety of zircon.
Gadolinite: essentially $Be_2FeY_2Si_2O_{10}$
Calciogadolinite (65): a calcian gadolinite.
Rowlandite: a silicate of yttrian earths.

[19] Most analyses of monazite show a range of 5 to 15 per cent of ThO_2. Higher concentrations are listed in the older literature (15), but these are likely to be erroneous in view of the difficulty of separating thorium from cerium. Gordon (31) has described a variety monazite from Llallagua, Bolivia, which is lacking in thorium.

[20] A titanian variety of thucholite has been described by Aminoff (1).

Hellandite: a rare earth silicate.
Johnstrupite: a rare earth silicate.
Mosandrite: a rare earth titano-silicate.
Cappelenite: a borosilicate of rare earths and barium.
Tscheffkinite: a rare earth titano-silicate.
Abukumalite (37): a silicophosphate of rare earths and calcium.
Kolm: a hydrocarbon containing traces of uranium.
Anthraxolite: a hydrocarbon containing traces of uranium.
Sphene: $CaTiSiO_5$.

References

1. Aminoff, G., Titanium thucholite from the Boliden Mine: *Geol. Fören. Förh.*, **65**, 31–36 (1943); *Chem. Abstr.*, **38**, 6244.
2. Bäckström, H., Bruno, C. A., and Müller, M., Investigation of the photographic latent image by means of the pressure effect: *The Svedberg, Uppsala* (**1944**), pp. 65–81.
3. Baranov, V. I., Zhdanov, A. P., and Deĭzenrot-Mysovskaya, M. Yu., Utilization of microradiographic methods for investigation of the distribution of radioactive elements in natural objects (in Russian): *Bull. acad. sci. U. S. S. R.; Classe sci. chim.* (**1944**), pp. 20–28.
4. Bardet, M. G., Essai de mesure de l'activite photographique de certains mineraux: *Bull. soc. min.*, **27**, 63 (1904).
5. Becquerel, H., Sur les radiations emises par phosphorescence: *Compt. rend.*, **122**, 420 (1896).
6. Behrens, B., and Baumann, A., Weitere Untersuchungen über die Verteilung des Bleis mit Hilfe der Methode der Autohistoradiographie: *Z. ges. exper. Med.*, **92**, 241–250 (1933).
7. Bespalov, M. M., Discovery of a new mineral of the thorianite group: *Soviet Geol.* (**1941**), no. 6, pp. 105–107; *Chem. Abstr.*, **38**, 4218.
8. Blau, M., Über das Abklingen des latenten Bildes bei Exposition mit alpha Partikeln: *Sitz. Akad. Wien., Math-Naturw. Klasse*, Abt. 2A, **140**, 623 (1931).
9. Blau, M., and Wambacher, H., Über den Einfluss des Kornzustands auf die Schwärzungsempfindlichkeit bei Exposition mit alpha Partikeln: *Z. wiss. Phot.*, **31**, 243 (1933).
10. Bragg, W. H., and Kleeman, R., On the alpha particles of radium and their loss of range in passing through various atoms and molecules: *Phil. Mag.* [6] **10**, 318 (1905).
11. Churchill, J. R., The formation of hydrogen peroxide during corrosion reactions: *Trans. Electrochem. Soc.*, **76**, 341–357 (1939).
12. Colson, R., Action du zinc sur la plaque photographie: *Compt. rend.*, **123**, 49–51 (1896).
13. Colson, R., Rôle des différentes formes de l'énergie dans le photographie au travers de corps opaques: *Compt. rend.*, **122**, 598–600 (1896).
14. Crookes, W., Radioactivity of uranium: *Proc. Roy. Soc. Lond.*, **66A**, 409–423 (1900).
15. Dana, E. S., *A System of Mineralogy*, 6th ed. with 3 app., John Wiley and Sons, New York (**1915**).
16. Danne, J., Sur un nouveau minéral radifère: *Compt. rend.*, **140**, 241 (1905).
17. Davis, C. W., The composition and age of uranium minerals from Katanga, South Dakota and Utah: *Am. J. Sci.* (5), **11**, 201–217 (1926).
18. Dersch, F., and Dürr, H., New method for the dry hypersensitization of photographic emulsions: *J. Soc. Mot. Pict. Eng.*, **28**, 178–187 (1937).
19. Doelter, C., and Leitmeier, H., *Handbuch der Mineralchemie;* uranium minerals, vol. 4 (**1928**); thorium minerals, vol. 3 [1], (1918). Dresden and Leipzig.

20. EASTMAN KODAK CO., *Photographic Plates for Use in Spectroscopy and Astronomy*, 5th ed. (**1943**), Rochester, N. Y.
21. ELLSWORTH, H. V., Rare-element Minerals of Canada: *Econ. Geol. Series*, No. **11**, Ottawa (1932).
22. EVANS, R. D., The measurement of natural alpha-particles ejected from solids: *Phys. Rev.*, **45**, 29–37 (1934).
23. EVANS, R. D., AND GOODMAN, C., Alpha-helium method for determining geological ages: *Phys. Rev.*, **65**, 216–227 (1944).
24. EVANS, R. D., HARRIS, R. S., AND BUNKER, J. W. M., Radium metabolism in rats and the production of osteogenic sarcoma by experimental radium poisoning: *Am. J. Roent. Rad. Therapy*, **52**, 353–373 (1944).
25. FRONDEL, C., NEWHOUSE, W. H., AND JARRELL, R. F., Spatial distribution of minor elements in single crystals: *Am. Mineral.*, **27**, 726–745 (1942).
26. GLEDITSCH, E., AND QVILLER, B., Investigation of uranothorites from the Arendal district, Norway: *Phil. Mag.* (7), **14**, 233 (1932).
27. GODDARD, E. N., AND GLASS, J. J., Deposits of radioactive cerite near Jamestown, Colorado: *Am. Mineral.*, **25**, 381–404 (1940).
28. GOLDSCHMIDT, V. M., Radioactivität als Hilfsmittel bei mineralogischen Untersuchungen: *Z. Kryst. Min.*, **44**, 545–560 (1908).
29. GOODMAN, C., AND PICTON, D. C., Autoradiography of ores: *Phys. Rev.*, **60**, 688 (1941).
30. GOODMAN, C., AND THOMPSON, G. A., Autoradiography of minerals: *Am. Mineral.*, **28**, 456 (1943).
31. GORDON, S. G., Thorium-free monazite from Llallagua, Bolivia: *Notulae Natural, Phil. Acad. Nat. Sci.*, no. 2, 7 pp. (**1939**).
32. GROVEN, C., GOVAERTS, J., AND GUÉBEN, G., Photographic action of artificial radioelements: *Nature*, **141**, 916 (1938).
33. HABERLANDT, H., Über die sogenannten Radiobaryte von Teplitz und Karlsbad: *Sitz. Akad. Wiss. Wien.*, Abt. IIa, **147**, 415 (1938).
34. HAHN, O., *Applied Radiochemistry*, Cornell Univ. Press, Ithaca (**1936**).
35. HAHN, O., KÄDING, H., AND MUMBRAUER, R., Die verschiedenen Arten der Abscheidung kleiner Substanzmengen in kristallisierenden Salzen und ihre photographische Sichtbarmachung: *Z. Krist.*, **87**, 387–416 (1934).
36. HAMILTON, J. G., SOLEY, M. H., AND EICHORN, K. B., Deposition of radioiodine in human thyroid tissue: *Univ. Cal. Pub. Pharmacol.*, **1**, no. 28, 339–368 (1940).
37. HATA, S., Abukumalite, a new yttrium mineral: *Sci. Papers Inst. Phys. Chem. Res. Tokyo*, No. 822, **34**, 1018–1023 (1938); abstr. *Am. Mineral.*, **24**, 66 (1939).
38. HOLMES, A., *Radioactivity and Geological Time*, Nat. Res. Council, Bull. No. 80, p. 159 (**1931**), Wash., D. C.
39. IIMORI, S., YOSHIMURA, J., AND HATA, S., Radioactive minerals from Shindem, Gifu prefecture: *Sci. Papers Inst. Phys. Chem. Res. Tokyo*, **20**, 485 (1934).
40. IIMORI, S., YOSHIMURA, J., AND HATA, S., A new radioactive mineral found in Japan: *Sci. Papers Inst. Phys. Chem. Res. Tokyo*, **15**, no. 285, 83–88 (1931).
41. KIMURA, K., The chemical investigations of Japanese minerals containing the rare elements: *Jap. J. Chem.*, **2**, 82–84, 84–85 (1925); abstr. *Am. Mineral.*, **11**, 137 (1926).
42. KIMURA, K., AND HIRONAKA, Y., Yamagutilite, a phosphorus-bearing variety of zircon found at Yamaguti village, Nagano prefecture: *J. Chem. Soc. Japan*, **57**, 1195 (1936); *Am. Mineral.*, **25**, 439 (1940).
43. KIMURA, K., AND MIYAKE, Y., On enalite, a new variety of uranothorite, found in Naegi, Gifu prefecture: *J. Chem. Soc. Japan*, **53**, 93 (1932).

44. KINOSHITA, S., The photographic action of the alpha particles emitted from radioactive substances: *Proc. Roy. Soc. London*, **83A,** 432–453 (1910).
45. KNOPF, A., The Age of the Earth; *Nat. Res. Council, Bull.* No. **80**, p. 6 (1931).
46. KURBATOV, I. D., KARZHAVINA, W. A., AND SAMOILO, N. A., Ionium in dispersed masses of Tyuya-Muyun: *Compt. rend. acad. sci. U. S. S. R.*, **1930A,** 69–74; *Chem. Abstr.*, **25,** 1731.
47. LACASSAGNE, A., AND LATTIS, J. S., Methode auto-histo-radiographique pour la détection dans les organes du polonium injecté: *Compt. rend.*, **178,** 488 (1924).
48. LACROIX, A., *Mineralogie de Madagascar*, vol. **3**, p. 309 (1923), Paris.
49. LARSEN, E. S., AND BERMAN, H., *The Microscopic Determination of the Nonopaque Minerals*, 2nd ed., *Bull.* **848,** *U. S. Geol. Survey*, Washington (1934).
50. LARSEN, E. S., JR., AND GONYER, F. A., Dakeite, a new uranium mineral from Wyoming: *Am. Mineral.*, **22,** 561–563 (1937).
51. LAUDA, J., Über das Abklingen des latenten Bildes auf der photographischen Platte: *Akad. Wiss. Wien., Math-Naturw. Klasse*, II-A, **145,** 707 (1936).
52. LEPIERRE, C., Yttrocolumbite de Mocambique: *Mem. Acad. Cien. Lisboa, Class Ciencias*, **1,** 369–375 (1937); *Am. Mineral.*, **25,** 155 (1940).
53. LIND, S. C., AND WHITTMORE, C. F., The radium-uranium ratio in carnotites: *Bur. Mines Tech. Paper*, No. **88,** Washington (1915).
54. LINDSAY, E., AND CRAIG, R., The distribution of radiophosphorus in insects: *Ann. Entomol. Soc. Am.*, **35,** 50 (1942).
55. MARBLE, J. P., A further study on the age of Great Bear Lake Pitchblende: *Am. Mineral.*, **22,** 564–566 (1937).
56. MCCOY, H. N., AND LEMAN, E. D., The relation between the alpha ray activities and ranges of radium and its short-lived products: *Phys. Rev.*, **6,** 184 (1915).
57. MCCOY, H. N., AND ROSS, W. H., The specific radioactivity of uranium: *J. Am. Chem. Soc.*, **29,** 1703 (1907).
58. MCCOY, H. N., AND ROSS, W. H., The relation between radioactivity and the composition of thorium compounds: *Am. J. Sci.*, **21,** 433 (1906).
59. MEES, C. E. K., On the resolving power of photographic plates: *Proc. Roy. Soc. London*, **83A,** 10 (1910).
60. MEIXNER, H., Fluoreszenzanalytische, optische und chemische Beobachtungen an Uranmineralen: *Chem. Erde*, **12,** 433–450 (1939–40).
61. MELON, J., La sharpite, nouveau carbonate d'uranyle du Congo belge: *Bull. Séan. Inst. Roy. Colon. Belge*, **9,** 333 (1938).
62. MISCIATELLI, P., Analysis of a radioactive pyromorphite from Gennammari, Sardinia: *Atti acad. Lincei*, **7,** 929–932 (1928).
63. MOSER, L., Über den Process des Schens und die Wirkung des Lichtsaufalle Körper: *Pogg. Ann.*, **56,** 177–234 (1842).
64. MUENCH, O. B., Sulfur in cyrtolite and its indication of galena: *Am. Mineral.*, **21,** 374 (1936).
65. NAKAI, T., On calcio-gadolinite, a new variety of gadolinite found in Tadati village, Nagano prefecture: *Bull. Chem. Soc. Japan*, **13,** no. 9, 591–594 (1938); *Am. Mineral.*, **25,** 312 (1940).
66. NEBLETTE, C. B., *Photography; its Principles and Practice*, 4th ed., D. Van Nostrand Co., Inc., New York (**1942**), p. 290.
67. NORTHROP, S. A., *Minerals of New Mexico*, Albuquerque (**1944**).
68. NOVÁČEK, R., Etudes sur quelques minéraux secondaires de l'uranium: *Mém. Soc. Roy. Sci. Bohême, Cl. 2* (**1935**), no. 7, 36 pp., 2 pls.; abstr. *Mineral. Abs.*, **6,** 148.

69. NOVÁČEK, R., The identity of dakeite and schroeckingerite: *Am. Mineral.*, **24,** 317–323 (1939).
70. PALACHE, C., BERMAN, H., AND FRONDEL, C., *Dana's System of Mineralogy*, 7th ed., vol. 1, John Wiley and Sons, Inc., New York (**1944**).
71. PECHER, C., Biological investigations with radioactive calcium and strontium: *Proc. Soc. Exptl. Biol. Med.*, **46,** 86 (1941).
72. PISANI, M. F., Examen de plusieurs mineraux au point de vue de leur radioactivite: *Bull. soc. min.*, **27,** 58 (1904).
73. RUSSELL, W. J., The action of certain substances on a photographic dry plate in the dark: *Phot. J.*, **23,** 91–97, 198–201, 231–234 (1898).
74. RUTHERFORD, E., CHADWICK, J., AND ELLIS, C. D., *Radiations from Radioactive Substances*, Macmillan Co., New York (**1930**).
75. RUTHERFORD, E., AND GEIGER, H., The number of alpha particles emitted by uranium and thorium and by uranium minerals: *Phil. Mag.* (6), **20,** 691 (1910).
76. SCHALLER, W. T., Rauvite from Temple Mt., Utah: *U. S. Geol. Survey, Bull.* **878,** p. 119, Washington (1937).
77. SCHNEIDERHÖHN, H., AND RAMDOHR, P., *Lehrbuch der Erzmikroskopie*, vol. 2, p. 519 (**1931**), Berlin, Gebrüder Borntraeger.
78. SCRIVENOR, J. B., AND SHENTON, J. C., Thorotungstite. A mineral containing tungsten and thorium from the Federated Malay States: *Am. J. Sci.*, (5), **13,** 487–490 (1927).
79. SHAPIRO, M. M., Tracks of nuclear particles in photographic emulsions: *Rev. Mod. Phys.*, **13,** 58 (1941).
80. SHORT, M. N., *Microscopic Determination of the Ore Minerals*, 2nd ed., *U. S. Geol. Survey, Bull.* **914,** Washington (1940).
81. SHOUPP, W. M., Phosphorus concentrates on steel blowhole surfaces: *Iron Age*, **148,** 51 (1941).
82. SIMPSON, E. S., Contributions to the mineralogy of Western Australia: *Proc. Roy. Soc. W. Australia*, **16,** 33–35 (1930–31); *Am. Mineral.*, **16,** 409, 472 (1931).
83. STARIK, I. E., KRAVCHENKO, L. L., AND MELIKOVA, O. S., A finding of ferrithorite in North Kirghizia: *Compt. rend. (Doklady) Acad. Sci. U. S. S. R.*, **32,** 254 (1941).
84. TAMMANN, G., Das Verhalten des Poloniums und des Thorium B zu anderen Metallen: *Z. Electrochem.*, **38,** 530 (1932).
85. THOMSON, J. J., On the effect of zinc and other metals on a photographic plate: *Proc. Camb. Phil. Soc.*, **9,** 372 (1897).
86. THOREAU, J., AND VAES, J. F., La saléite, nouveau minéral uranifère: *Bull. Soc. Belge Géol.*, **42,** 96 (1932).
87. TYLER, S. A., AND MARAIS, J. J., A method for the determination of the relative radioactivity of mineral grains: *J. Sedimentary Petrol.*, **11,** 145–147 (1941).
88. VAES, J. F., Sur un minéral de Kalongewe (Katanga): *Ann. Soc. Géol. Belgique*, **56,** B331–2 (1933).
89. VON GROSSE, A., On the origin of the actinium series of radioactive elements: *Phys. Rev.*, **42,** 42, 565 (1932).
90. WAMBACHER, H., Untersuchung der photographischen Wirkung radioaktiver Strahlungen auf mit Chromsäure und Pinakryptolgelb vorbehandelten Filmen und Platten: *Sitz. Akad. Math-Naturw. Klasse, Abt. 2A*, **140,** 271 (1931).
91. WHERRY, E. T., Radioactive minerals found in Pennsylvania and their effect on the photographic plate: *J. Franklin Inst.*, **165,** 57–78 (1908).
92. WILKINS, T. R., The response of photographic materials to atomic particles: *J. Applied Phys.*, **11,** 35–45 (1940).

93. WILKINS, T. R., Cosmic ray tracks in photographic emulsions: *Nat. Geog. Soc. Stratosphere Series*, **2,** 37 (1936).
94. YAGODA, H., Analytical patterns in the study of mineral and biological materials: *Ind. Eng. Chem., Anal. ed.*, **15,** 135 (1943).
95. YAGODA, H., Luminescent phenomena as aides in the localization of minerals in polished in sections: *Econ. Geol.*, **40,** 97 (1945).
96. YAGODA, H., The localization of copper and silver sulfide minerals in polished sections by the potassium cyanide etch pattern: *Am. Mineral.*, **30,** 51–64 (1945).